MADLab
Mechanics, Acoustics, and Dynamics Lab

Sound absorption properties of additively manufactured porous materials with minimal surface pore geometries

Anthony Ciletti[1], Martha C Brown[2], Janith Godakawela[3], and Bhisham Sharma[3]

[1]Aerospace Engineering, Wichita State University, Wichita, KS, United States
[2]Aeroacoustics Branch, NASA Langley Research Center, Hampton, VA, United States
[3]Mechanical Engineering – Engineering Mechanics, Michigan Technological University, Houghton, MI, United States

Evolution of Aircraft Engine Noise

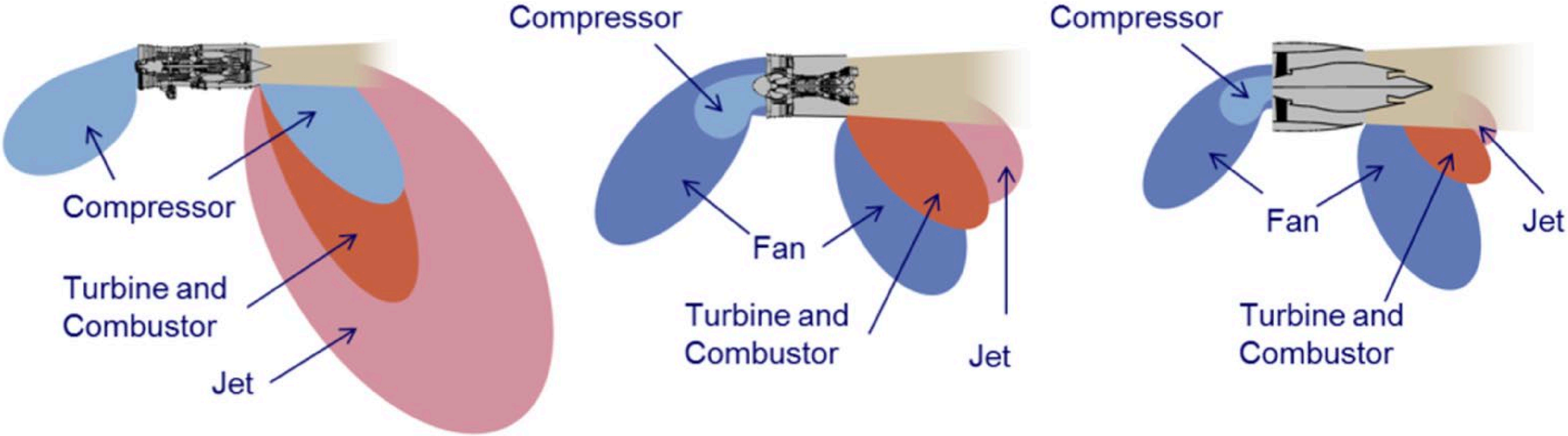

1960s
1:1 BPR Engine

1990s
6-8:1 BPR Engine

2000s
12:1 BPR Engine

The evolution of the relative dominance of various acoustic sources as the engine bypass ratio (BPR) has increased.

Source: Epstein, Alan, "The Lessons of P&W's Geared Turbofan Engine and the Implications for the Future," Keynote Address, International Symposium on Air Breathing Engines (ISABE), Phoenix, AZ, October 2015.

State-of-the-Art Noise Reduction Solutions

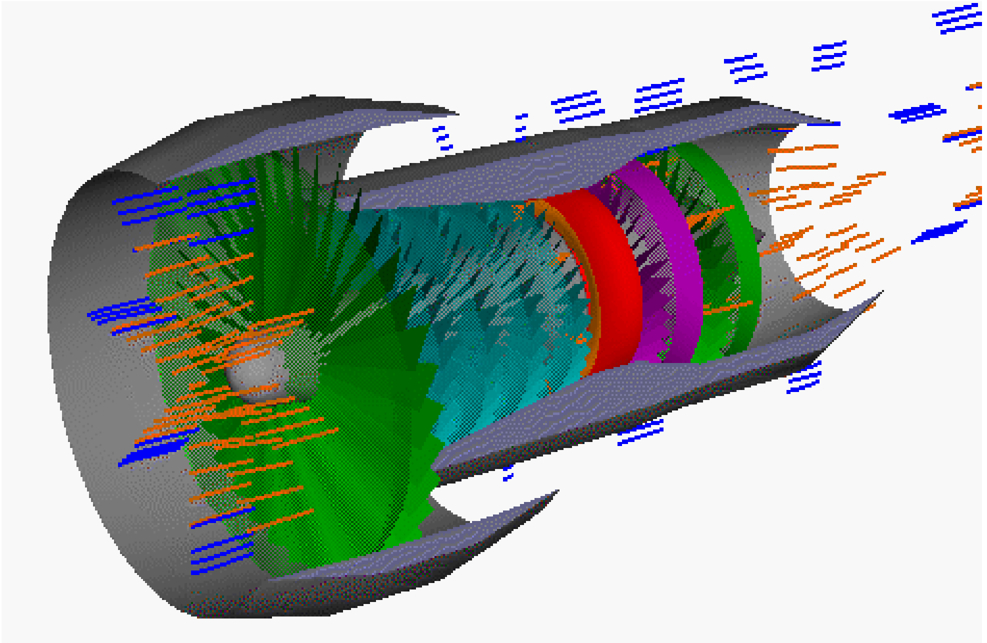

Source: Van Zante et al. "Propulsion Noise Reduction Research in the NASA Advanced Air Transport Technology Project" NASA Technical Report (2017)

Multiple DOF Liners

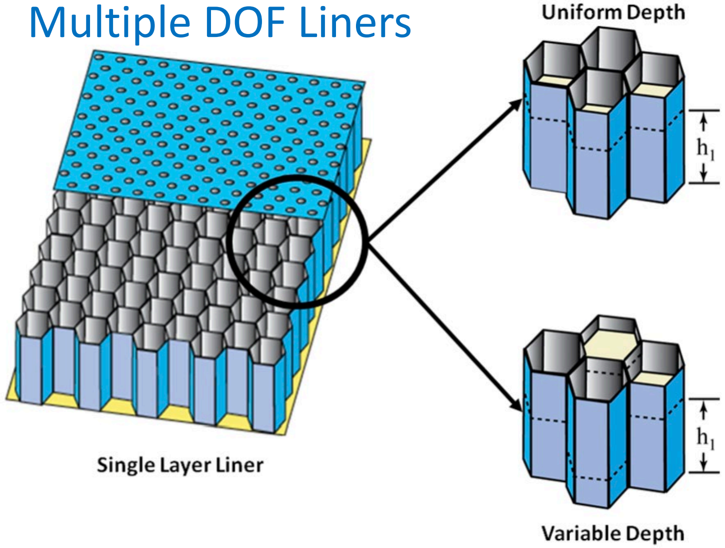

Over the Rotor Foam Metal Liners

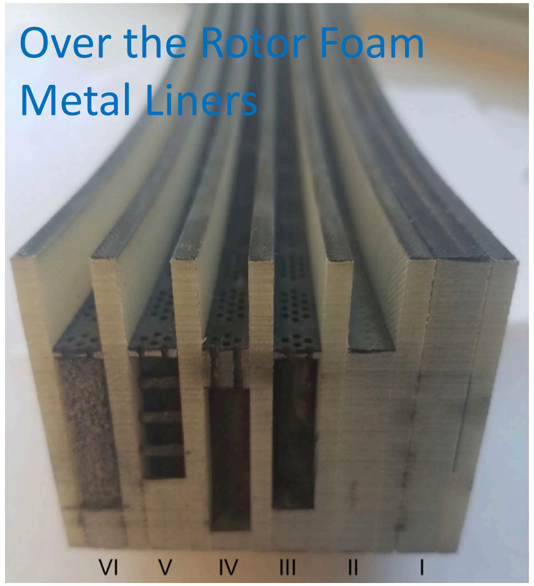

Soft Stator Vanes

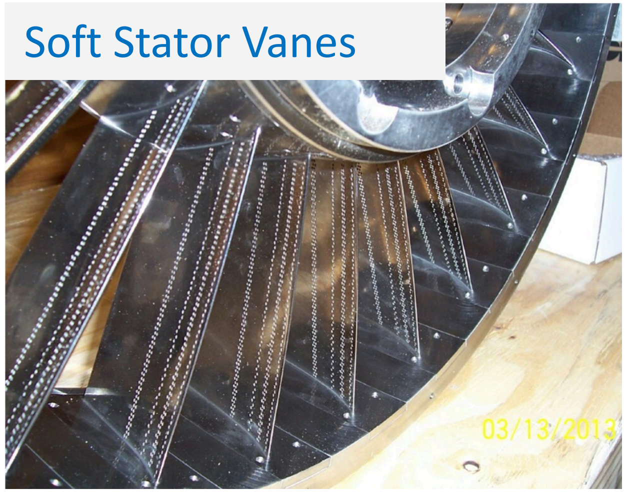

Serrated Trailing Edge (NASA GRC)

Marcelled Trailing Edge (GE)

Current Broadband Acoustical Materials

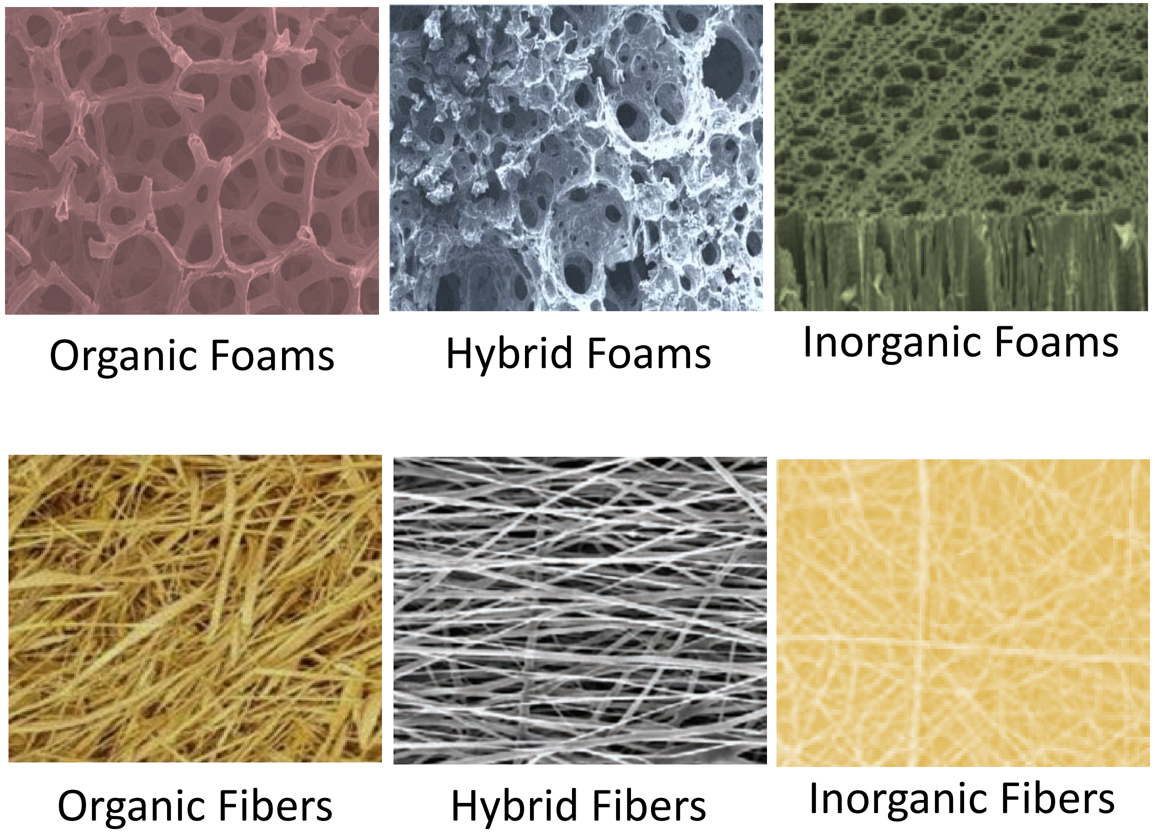

Various types of commonly used porous acoustical materials.

Conventional bulk absorbers

- Underlying porous architecture is *incidental* to the fabrication process.
- Fabrication methods limit:
  - x Microstructural optimization
  - x Material optimization
  - x Functionality optimization

Triply Periodic Minimal Surfaces

- Minimal Surface: Surface with zero mean curvature
- TPMS: Minimal and periodic in three directions

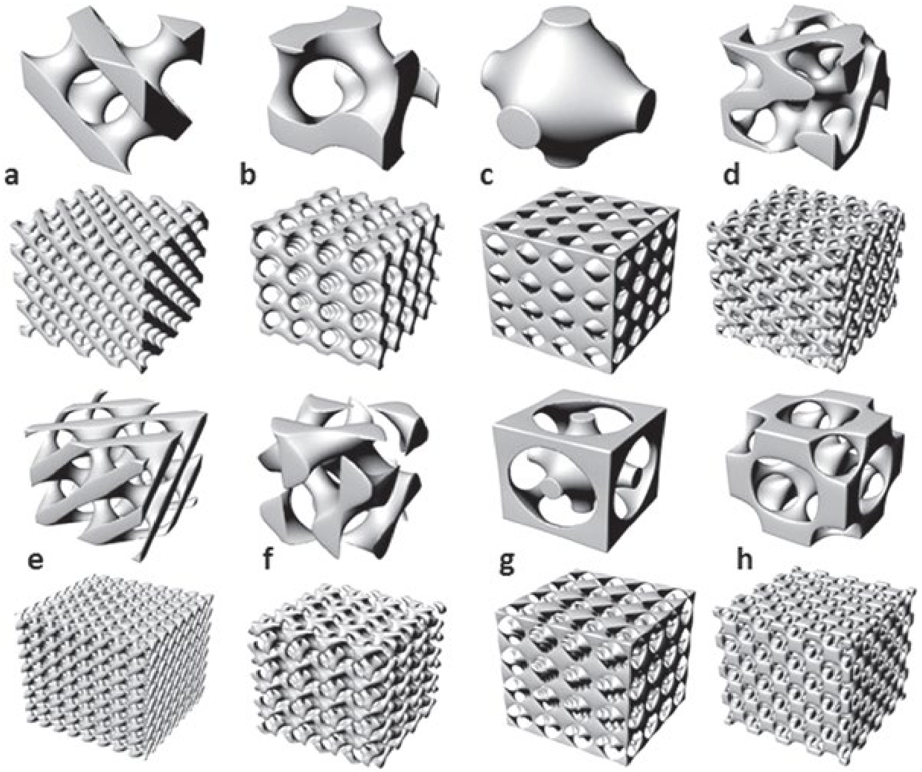

Different TPMS unit cells and structures

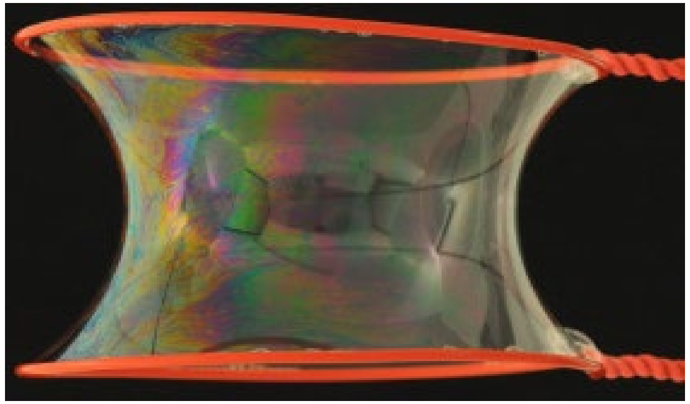

Nature often seeks optimal forms in terms of perimeter and area such as minimal surfaces

Triply Periodic Minimal Surfaces Structures

Potential multifunctionality

Load bearing + Thermal management + Energy Absorption + *Acoustic Absorption?*

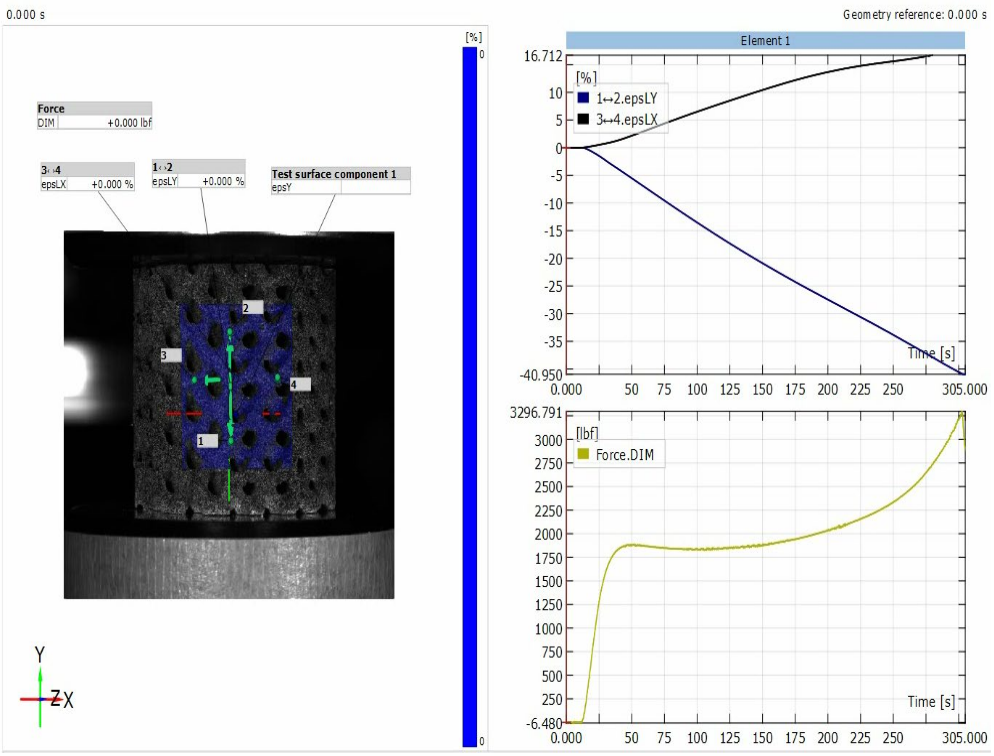

Energy absorption behavior of a gyroid structure*

*Ref: W. Johnston, et al. “Fibro-Porous Materials: 3D Printed Hybrid Acoustical Materials for Multifunctional Applications” under review.

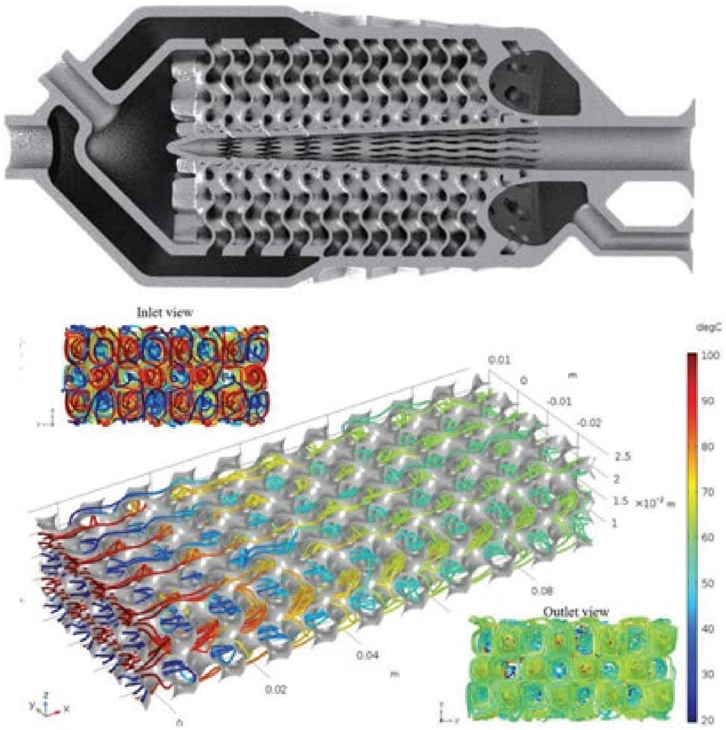

TPMS heat exchangers#

#Ref: nTopology.com

Sample Selection and Fabrication

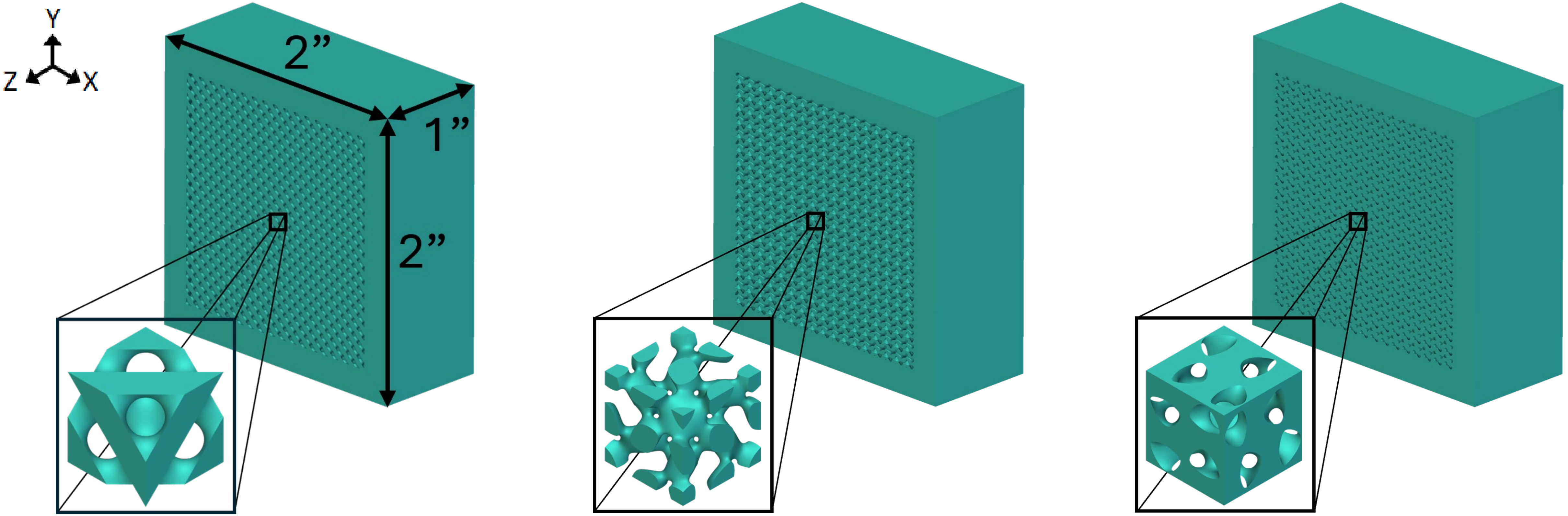

Diamond

Lidinoid

Split-P

- All samples were fabricated using vat photopolymerization (Form 3+ and Clear resin)
- Samples were printed with porosities of 20%, 40%, 60% for each TPMS type

Normal Incidence Testing

Testing conducted using NIT setup at NASA Langley

Unique Capabilities:

- Sound pressure level (SPL) up to ~155 dB
- Sound Source: tonal (stepped-sine, swept-sine, multi-tone) and broadband
- Frequency range of 400 to 3000 Hz

Rotating Plug

Two measurement microphones positioned 2.5 in. and 3.75 in. from the liner surface and mounted so their positions can be precisely interchanged by rotating the plug 180°. This two-microphone method eliminates the need for precise amplitude and phase calibrations.

Reference Microphone

Located 0.25 in from the surface of a liner is used to determine the surface sound pressure level (SPL)

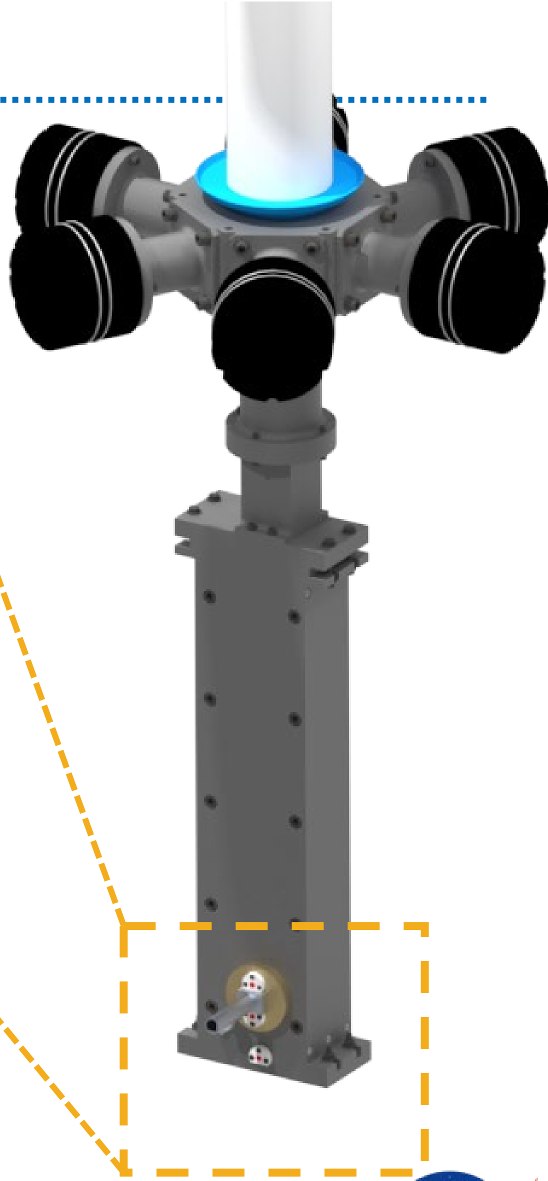

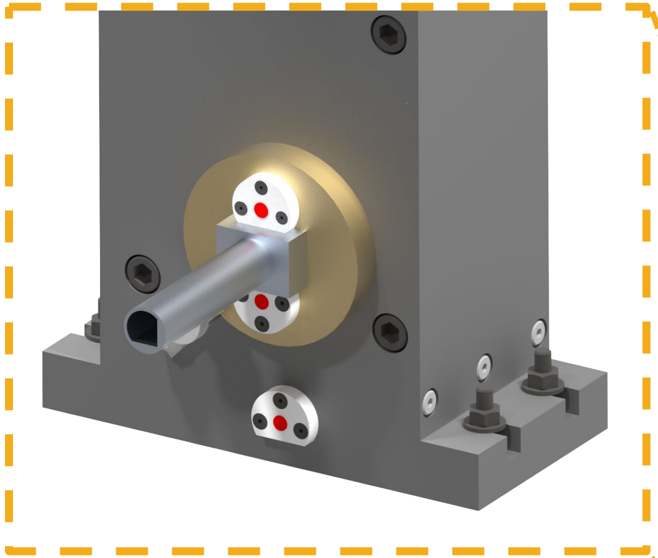

Sample Installation

Sample holder can accommodate 2 by 2 in. liner samples up to 12 in. thick

Airflow Resistance Testing

Testing conducted using Raylometer at NASA Langley

Measures the steady or DC flow resistance across a sample.

Unique Capabilities:

- Controlled velocities of 0.2 to 500 cm/s
- Samples tested include: perforates, microperforates, wire mesh, and bulk absorbers.

Upstream/Downstream Spiral Static Pressure Array
20 static pressure ports correct for nonuniform near-field effects close to sample.

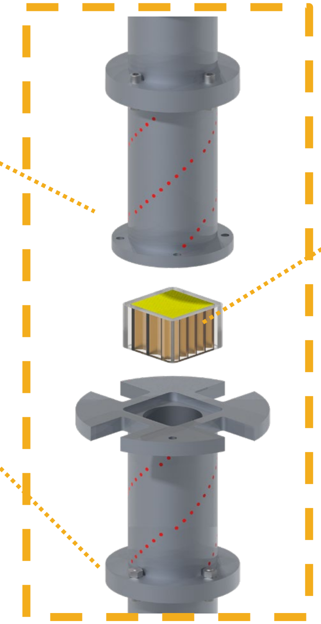

Sample Section
Has the ability to test 2 in by 2 in square, or 2.25 in diameter sample sizes.

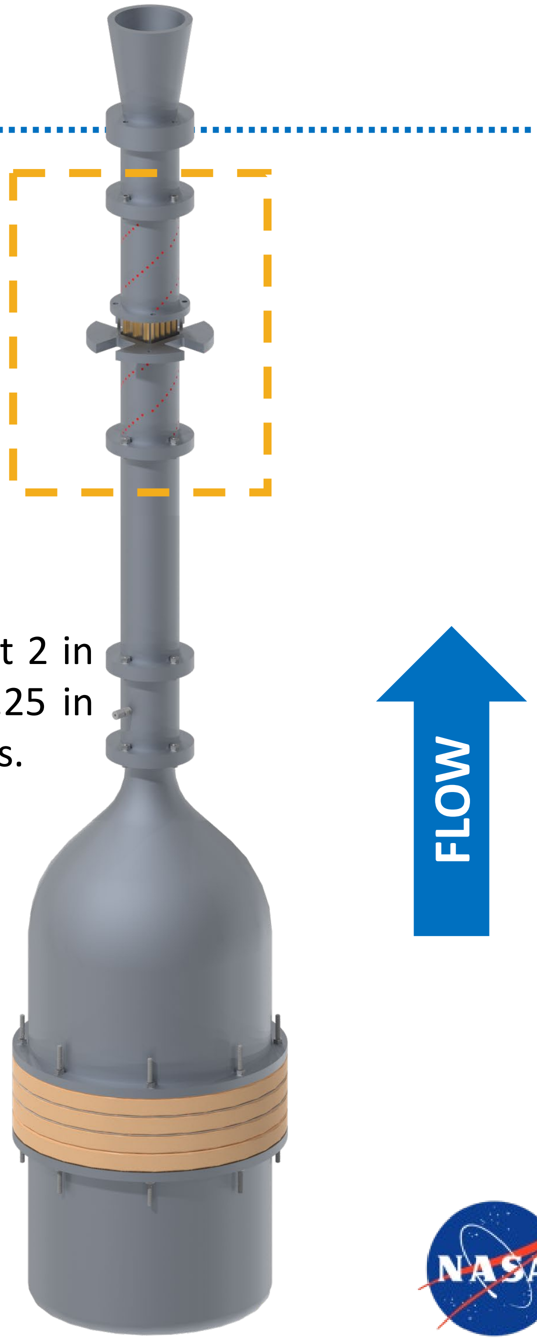

$$\frac{R_f}{\rho c} = \frac{\Delta P}{\rho c U} \rightarrow \theta \text{ at 0 Hz}$$

Normal Incidence Acoustic Measurements

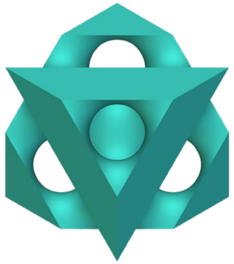

Diamond

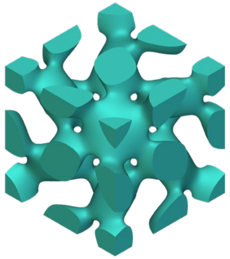

Lidinoid

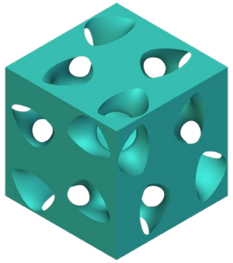

Split-P

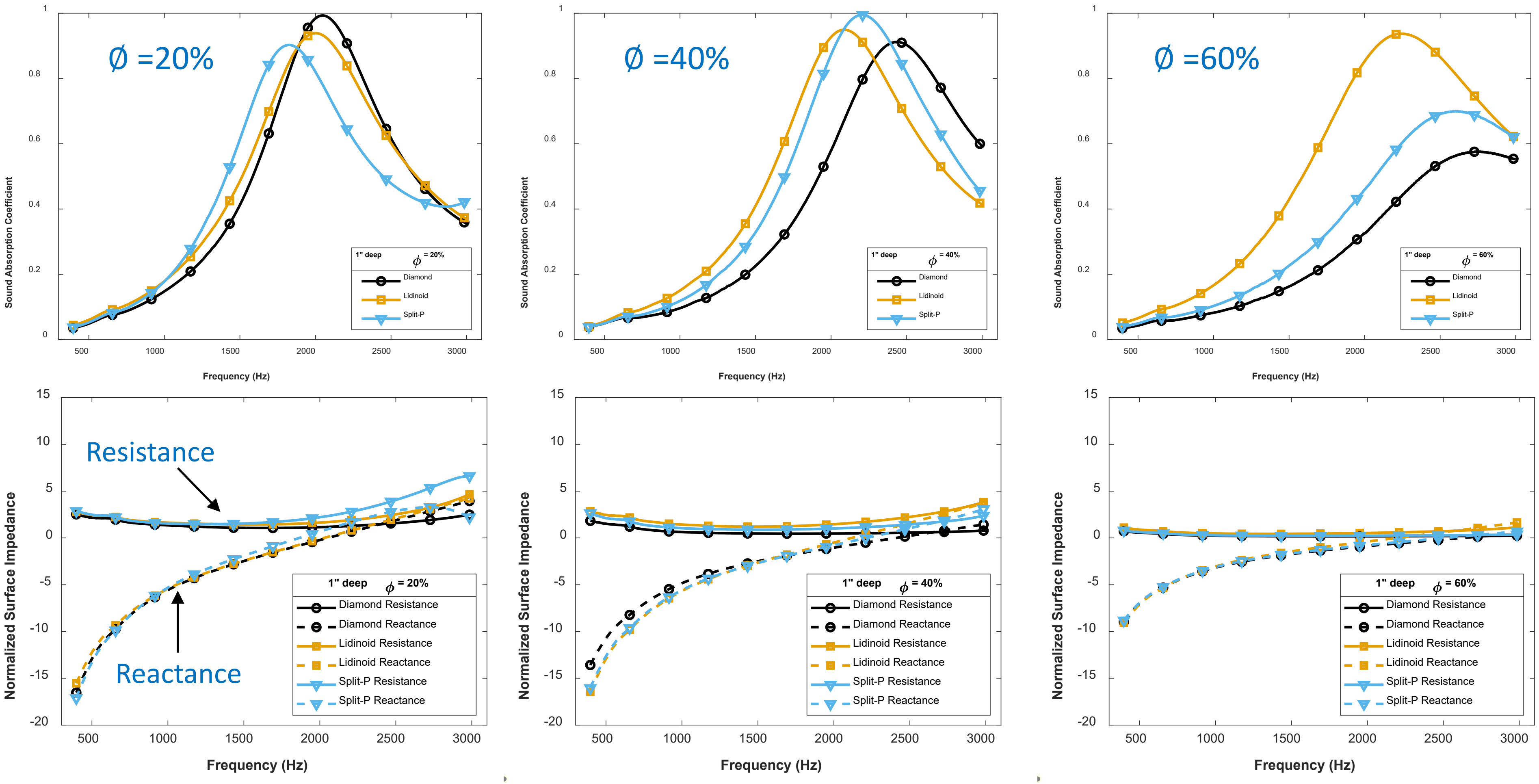

Measured sound absorption (top row) and normal impedances (bottom row) for all fabricated samples

Numerical Modeling

Inverse Characterization

- Five-parameter Johnson-Champoux-Allard (JCA) formulation.
  - Open porosity (φ)
  - Tortuosity (α_∞)
  - Static airflow resistivity (σ)
  - Viscous characteristic length (Λ)
  - Thermal characteristic length (Λ')
- Complex effective density:

$$\tilde{\rho} = \frac{\rho_0 \alpha_\infty}{\phi}\left(1 + \frac{\phi\sigma}{j\omega\rho_0\alpha_\infty}\left(1 + j\frac{4\omega\rho_0\eta\alpha_\infty^2}{\sigma^2\phi^2\Lambda^2}\right)^{\frac{1}{2}}\right)$$

- Effective bulk modulus:

$$\tilde{K} = \frac{\gamma P_0/\phi}{\gamma - (\gamma - 1)\left(1 + \frac{8\eta}{j\omega B^2\Lambda'^2\rho_0}\left(1 + j\frac{\omega B^2\Lambda'^2\rho_0}{16\eta}\right)^{\frac{1}{2}}\right)^{-1}}$$

Transfer Matrix Method

- For each porous layer:

$$\mathbf{T} = \begin{bmatrix} \cos(kd) & j\frac{\omega\tilde{\rho}}{k}\sin(kd) \\ j\frac{k}{\omega\tilde{\rho}}\sin(kd) & \cos(kd) \end{bmatrix}$$

- Global transfer matrix in stacked configurations: $\mathbf{T}^G = [\mathbf{T}^1][\mathbf{T}^2][\mathbf{T}^3] \dots [\mathbf{T}^i] \dots [\mathbf{T}^n]$
- In parallel layers: $Z^i = \frac{2}{\frac{1}{Z_1^i} + \frac{1}{Z_2^i}}$

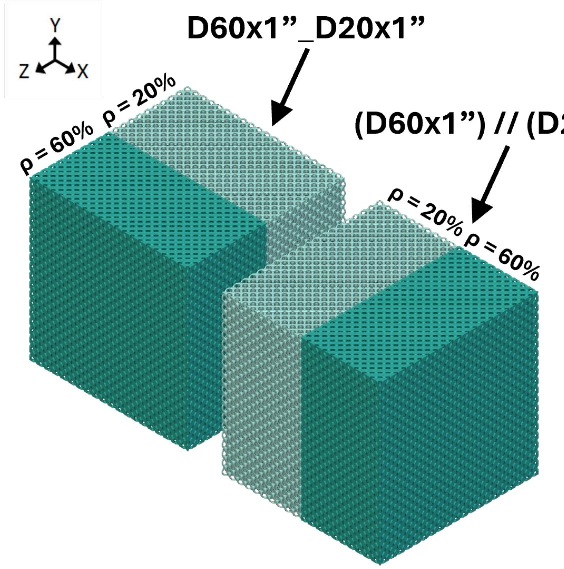

Layered Configurations

Fitting Predictions

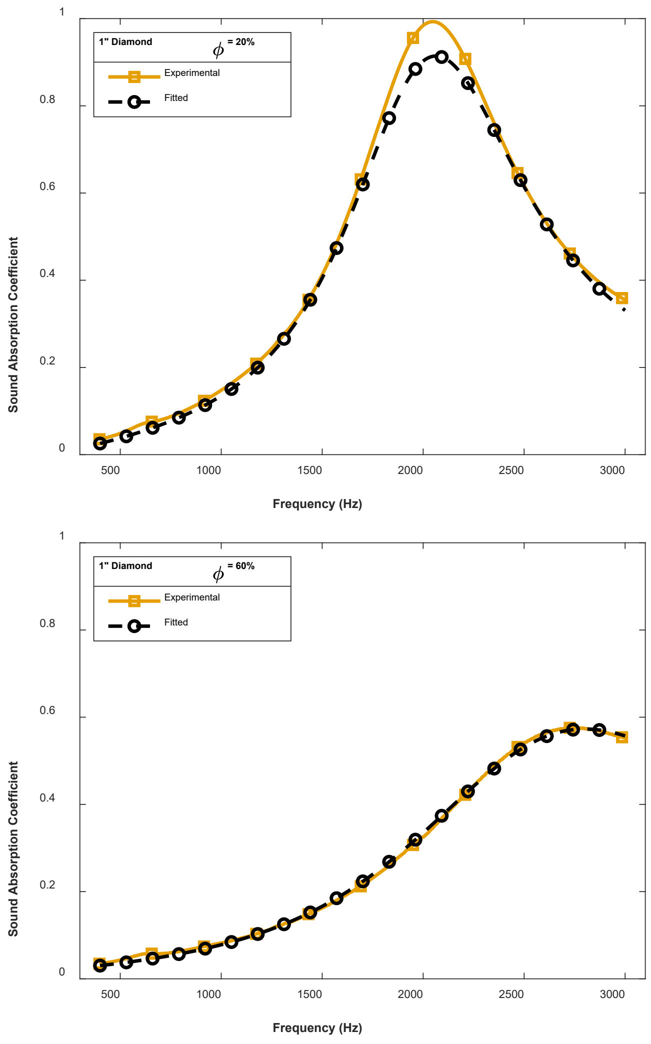

Measured v/s fitted absorption

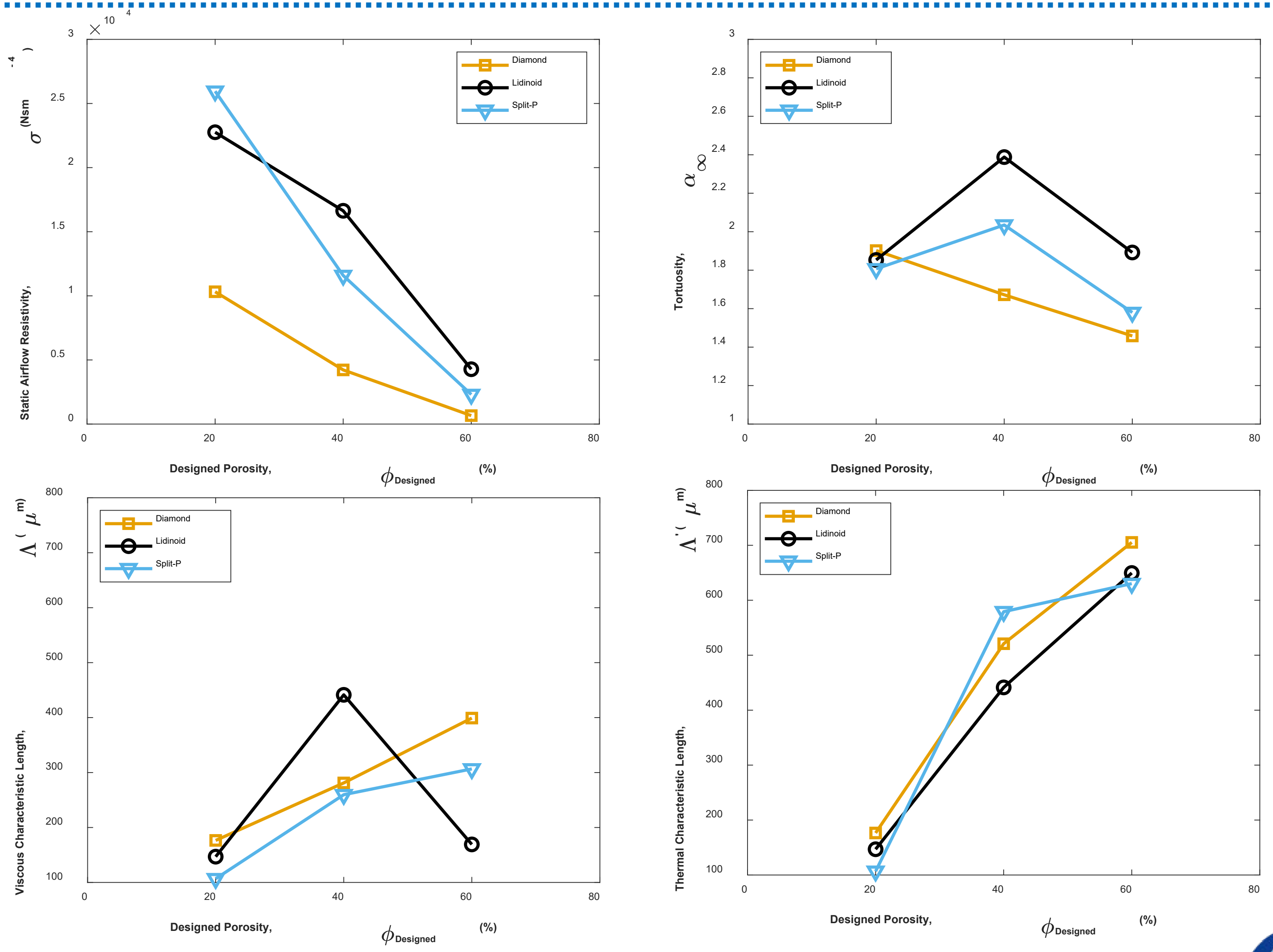

Inversely characterized bulk transport parameters

Performance Tailoring

Layered Configurations

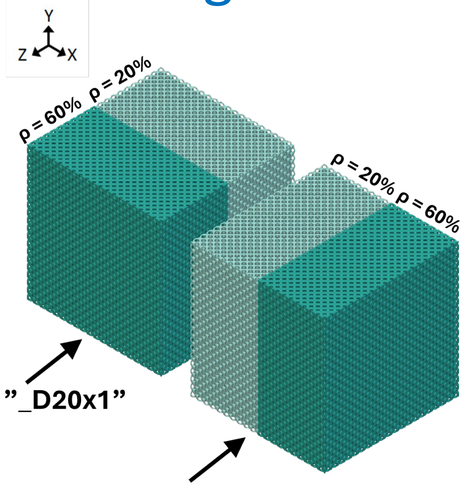

D60x1"_D20x1"

(D60x1") // (D20x1")

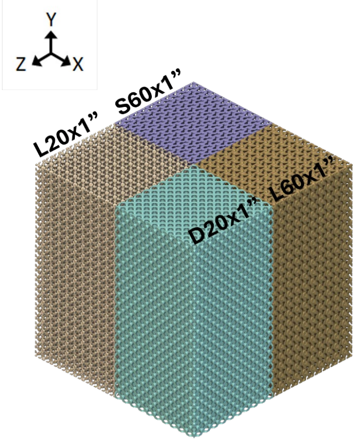

(L20x1"_S60x1") // (D20x1"_L60x1")

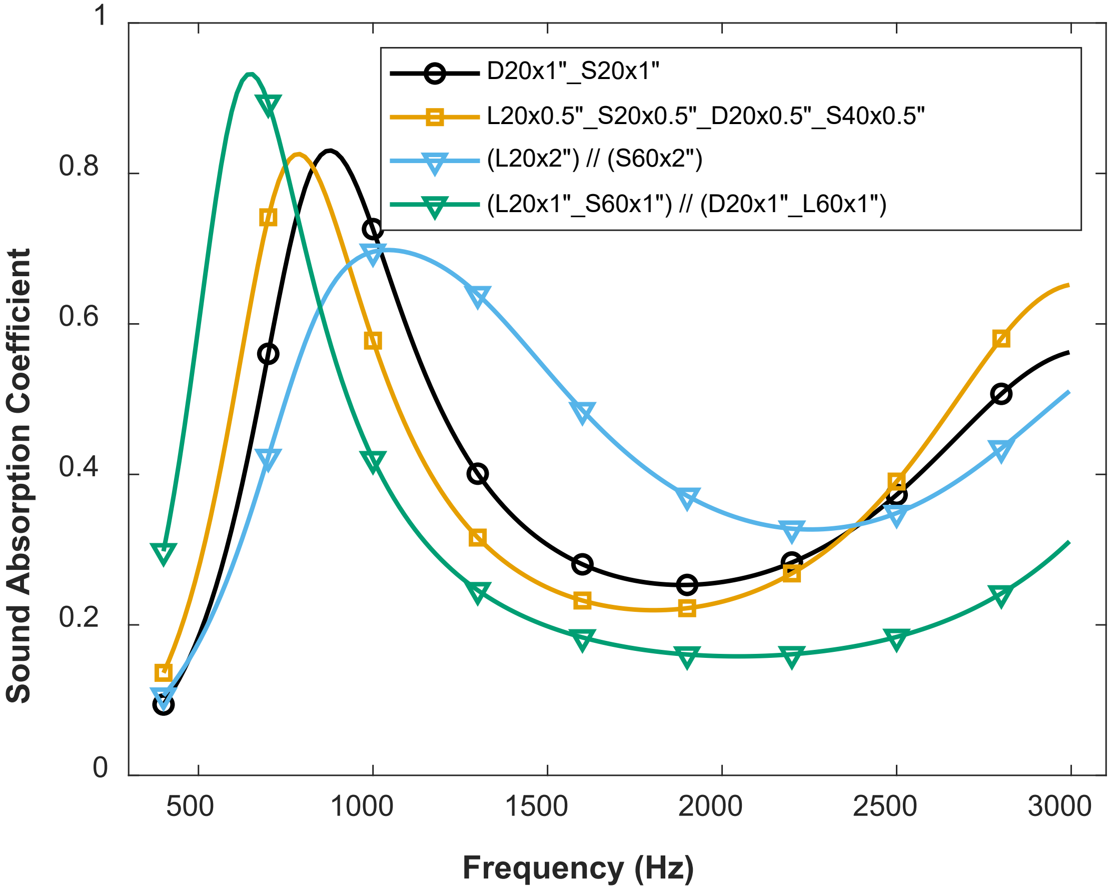

Sound absorption performance predictions for various layered configurations obtained using the transfer matrix method

Conclusions

- The sound absorption properties of three TPMS-based porous structures were studied: Diamond, Lidinoid, and Split-P.
- Diamond samples were found to be easiest to print and Lidinoid samples were found to be the most difficult to print using vat photopolymerization.
- All three geometries show increasing absorption with reduced porosity.
- The absorption increase is primarily driven by increase in flow resistance and relatively high tortuosity values.
- The absorption behavior can be modeled using the inverse characterization technique and the JCA rigid model.
- A transfer matrix approach enables the design of layered absorbers with performance-tailored sound absorption.

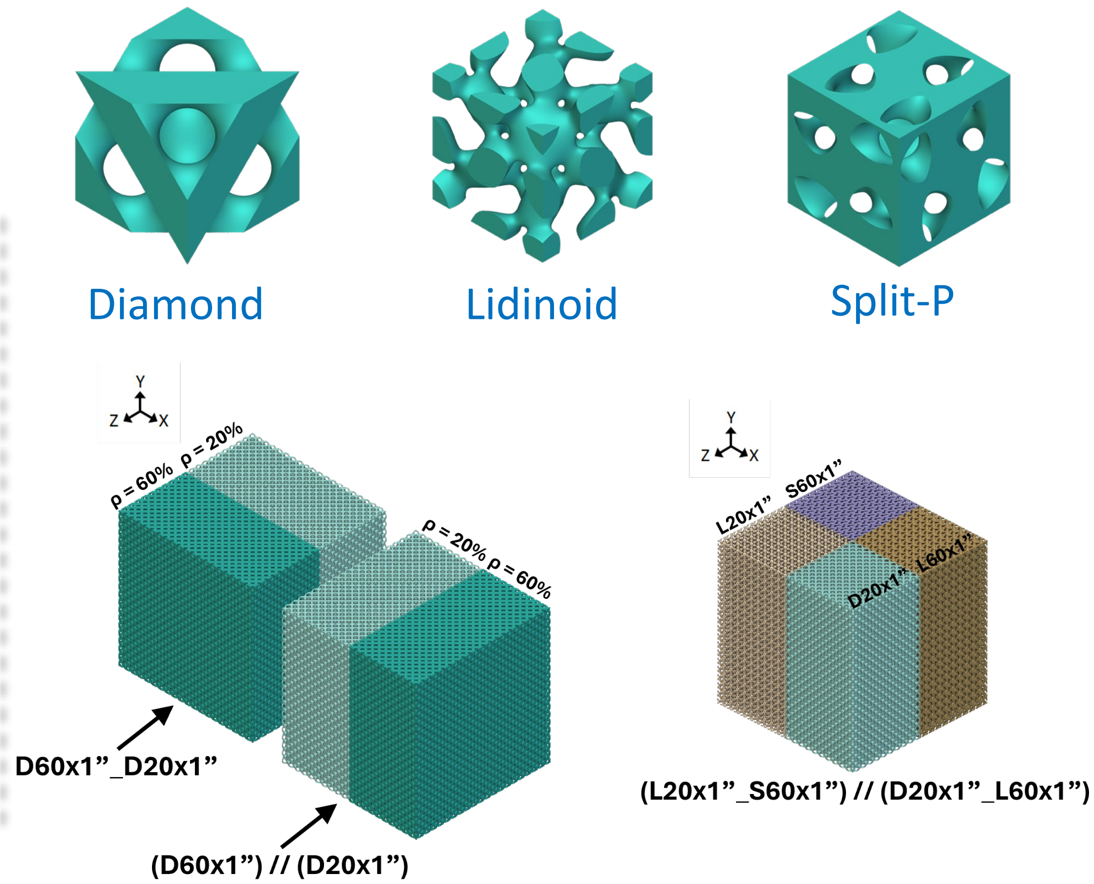

Acknowledgments

- Anthony Ciletti would like to acknowledge funding support from the NASA Advanced Air Transport Technologies Project of the Advanced Air Vehicles Program